

Bactericidal action of cold atmospheric plasma in solution

V Boxhammer^{1,4}, G E Morfill¹, J R Jokipii², T Shimizu¹,
T Klämpfl¹, Y-F Li¹, J Köritzer¹, J Schlegel³
and J L Zimmermann¹

¹ Max Planck Institute for Extraterrestrial Physics, Garching, Germany

² Lunar and Planetary Laboratory, University of Arizona, Tucson, AZ, USA

³ Department of Neuropathology, Technical University Munich, Munich, Germany

E-mail: boxhammer@mpe.mpg.de

New Journal of Physics **14** (2012) 113042 (18pp)

Received 10 August 2012

Published 29 November 2012

Online at <http://www.njp.org/>

doi:10.1088/1367-2630/14/11/113042

Abstract. In this study different influences on the bactericidal effect of cold atmospheric plasma (CAP) were investigated intensively. In detail, different initial densities of *Escherichia coli* cells and different treatment times of up to 8 min were studied. The results show that up to densities of 10^5 cells per $20 \mu\text{l}$ high reduction rates of up to 5 log can be achieved in less than 3 min of CAP application. In contrast, for higher cell densities almost no reduction was measured for CAP treatment times of up to 8 min. To understand this data in detail, a theoretical model was developed. This model starts from the premise that bacteria are able to some degree to neutralize reactive species and that accordingly the bactericidal effect depends on the bacterial concentration. A further purpose of this study was to analyze the contribution of reactive oxygen and also reactive nitrogen species—produced by the CAP—to the bactericidal effect. We therefore measured nitrites, nitrates and hydrogen peroxide—products of chemical reactions between the species produced by the CAP and the liquid. The evidence of nitric oxide (NO) uptake in bacteria and the corresponding reference experiments with hydrogen peroxide and a chemical NO donor clearly

⁴ Author to whom any correspondence should be addressed.



Content from this work may be used under the terms of the [Creative Commons Attribution-NonCommercial-ShareAlike 3.0 licence](https://creativecommons.org/licenses/by-nc-sa/3.0/). Any further distribution of this work must maintain attribution to the author(s) and the title of the work, journal citation and DOI.

show that the bactericidal effect of CAP is related to a combination of oxidative and nitrosative effects.

Contents

1. Introduction	2
2. Experimental setup	3
2.1. Plasma device	3
2.2. Bacterial strains and growth conditions	4
2.3. Plasma application and experimental setup	5
2.4. Performance of cell number tests	5
2.5. Detection of reactive oxygen species: Amplex [®] Red Hydrogen Peroxide Assay	5
2.6. Detection of reactive nitrogen species	5
2.7. Reference experiments with hydrogen peroxide (H_2O_2) and nitric oxide (NO)	6
2.8. Fluorescence proof of intracellular NO	6
3. Results and discussion	6
3.1. Cell number tests	6
3.2. Peroxides in liquids	6
3.3. Nitrates and nitrites in liquids	7
3.4. Combination of NO and H_2O_2	8
3.5. Direct evidence of NO in cells	8
3.6. Bacteria in solution—model	9
3.7. Discussion and conclusions	15
Acknowledgments	16
References	17

1. Introduction

Cold atmospheric plasma (CAP) is one of the most promising prospective tools for the prevention of infectious diseases and nosocomial infections. It is known that CAPs inactivate a wide range of microorganisms like bacteria, fungi, biofilms, viruses and spores [1–6]. A very crucial point is that CAPs are also able to inactivate bacteria resistant to antibiotics like *multi-resistant Staphylococcus aureus (MRSA)* [7, 8]. Even *Deinococcus radiodurans* which is resistant against ultraviolet (UV) radiation, oxidation and desiccation—making it ‘the world’s toughest bacterium’, as stated in the Guinness Book of World Records—can be inactivated within a few seconds [9]. Recent results furthermore show that microorganisms can also be inactivated through different textiles which opens up even more application areas [10]. Although intensive research has been performed in the past years, the exact bactericidal mechanisms of CAPs are still not fully understood yet. However, the current state of the art is that there are several processes which contribute to the inactivation of microorganisms [11–13]. Intensive investigations in the past lead to the assumption that reactive species (besides charged particles) play the most important role in inactivation [12–19]. Some investigators were able to show morphological changes in bacterial structures after the CAP application [11, 20, 21]. This loss in membrane integrity is believed to be caused by the generation of reactive oxygen species (ROS) and the resulting lipid peroxidation. This is a very important result as it shows that the

whole cell wall of the bacteria breaks due to the CAP treatment [21]. Due to these experimental results most of the recent studies focused on occurring ROS and yielding peroxides during the CAP application leading to oxidative stress on the microorganisms. This is of substance as most of the pathogenic microorganisms do not possess any adequate defending systems against oxygen [22]. Nevertheless it has to be pointed out that, for example, Gram positive bacteria are not as susceptible to oxidative damage as Gram negative bacteria but studies using CAP showed that even Gram positive bacteria (like MRSA) could be easily inactivated within seconds [7, 23].

To produce plasma at atmospheric pressure different investigators and groups developed different technologies using different carrier gases, plasma parameters, etc. The end product is always CAP. Nevertheless depending on the different above mentioned parameters the compositions and also the concentrations of the produced electrons, charged particles, reactive species, etc vary considerably.

The CAP device used for this study produces plasma by using the surface micro discharge (SMD) technology in air [1]. Therefore besides electrons, charged particles and UV light, reactive species—mainly reactive oxygen and reactive nitrogen species—are also produced.

As the bacterial load in the fluid of chronic wounds plays a major role in the healing process, the influence of the initial cell density in solution on the bactericidal efficacy of the CAP treatment was investigated in detail. To get a deeper insight into the observed density effects a theoretical model was developed, which relates the bactericidal efficacy to bacterial density and treatment time.

Furthermore products of dissolved reactive species were monitored in liquid to analyze the relationship between increasing content of all reactive species—not only oxygen but also nitrogen species—on the bactericidal efficacy of CAP.

2. Experimental setup

2.1. Plasma device

The CAP device employed in this study utilizes the SMD technology to produce the plasma which has been published and characterized in detail in Morfill *et al* [1] and Maisch *et al* [3]. In short, the electrode for plasma production is located at the top inside a closed box made out of Teflon (figure 1). The electrode itself consists of a Teflon plate which is sandwiched by a brass planar plate and a stainless steel mesh grid. A high sinusoidal voltage of 8.5 kV_{pp} with a frequency of 1 kHz is applied between the brass plate and the mesh grid to produce a homogenous plasma by many micro-discharges in the ambient air (blue light in figure 1). The power consumption for the plasma discharge equals 0.02 W cm^{-2} and was evaluated by the Lissajous figure method using a $1 \mu\text{F}$ capacitor [24].

The samples to treat were directly placed beneath the plasma electrode. The door of the CAP device was closed during the complete treatment—thereby closing up the treatment volume.

As already mentioned in the introduction, the CAP used in this study produces electrons, charged particles, reactive species (mainly reactive oxygen and nitrogen species), UV light and heat. Details have been published in Maisch *et al* [3]. In short, the amount of charged particles (electrons and ions) at the surface of the electrode was measured to $\sim 10^{11} \text{ cm}^{-3}$. Nevertheless due to excitation, dissociation, attachment and recombination processes the density of charged

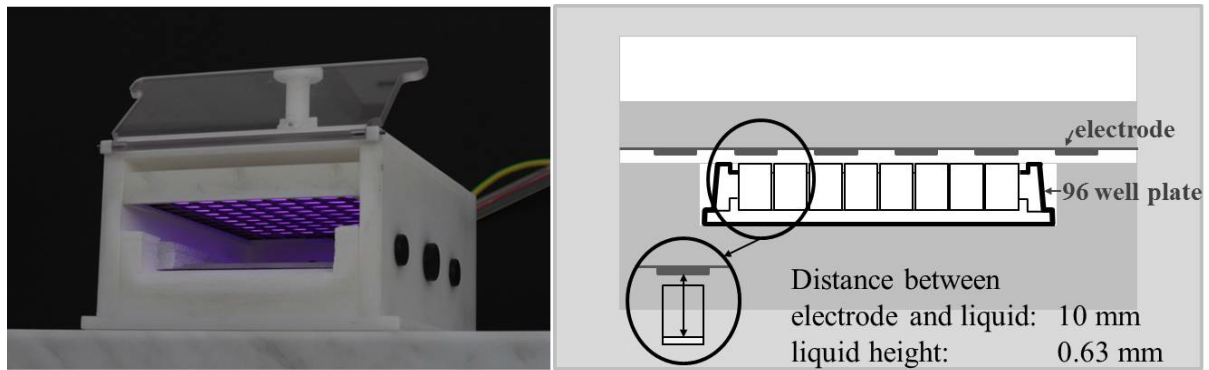


Figure 1. CAP device, based on the SMD technology, used for this study. The samples to treat were placed directly beneath the electrode. The position of the electrode is adjustable and was kept at 1 mm above the plate. The door of the device was closed during the CAP treatment, so that the species produced by the plasma were confined inside.

particles which reach the sample is low (by comparison with the density at source). Concerning the measurement of reactive species, ozone, nitric oxide (NO) and nitrogen dioxide reached values of ~ 500 , <1 and ~ 3 ppm. The UV light emitted by the CAP is mainly observed from the N_2 positive system between 280 and 420 nm in wavelength. Furthermore peaks in the UVC region of the spectrum resulting from the NO γ system can be detected. The UV power density measured with a power meter (HAMAMATSU UV-Power Meter C8026, Japan) equalled 25 nW cm^{-2} . This value is far below ICNIRP (International Commission Non-Ionizing Radiation Protection) safety levels. Due to the fact that the CAP device is an indirect plasma source, the electric current is estimated small (below 0.1 mA) since almost no charged particles can reach the sample. Furthermore any kind of temperature effects can be ruled out, as a maximum 4°C above the ambient temperature was reached (average temperature, monitored by a thermocouple, K102 thermocouple; Voltcraft, Germany)—even for longer electrode operation times. Nevertheless by increasing the ambient temperature and in addition the relative humidity—by, for example, placing liquid samples in the closed volume of the CAP device—the concentration of water vapour can be significantly increased and therefore the production of hydroxyl radicals may be expected to be correspondingly higher. However, previous experiments using different ambient conditions ($15\text{--}35^\circ\text{C}$ in temperature and $20\text{--}80\%$ in humidity) did not show any significant impact on the bactericidal property of the CAP device [25].

2.2. Bacterial strains and growth conditions

A standard strain of *Escherichia coli* (*E. coli*), ATCC 9637, was used for all experiments. Results of the experiments were also confirmed with a standard Gram positive strain of *Staphylococcus capitis* (*S. capitis*), DSM 20326, but were not included in this manuscript as they do not provide any additional information. Nevertheless they support our findings. *E. coli* were grown aerobically at 37°C in lysogeny broth medium (*S. capitis* in soy broth) to mid-exponential phase (estimated via optical density at $600 \text{ nm} = \text{OD}_{600}$).

2.3. Plasma application and experimental setup

In the setup used in this study, bacteria were treated with the above mentioned CAP device in 20 μ l of Tris buffered saline (TBS, pH 7.6) in wells of a 96 well plate. The 96 well plate was treated with CAP with a distance between the electrode and liquid surface of \sim 10 mm. The liquid height in the well was \sim 0.63 mm. All experiments were carried out in triplicate for at least three times.

2.4. Performance of cell number tests

The bacterial colony count assay is the standard way to assess the bactericidal property of an antimicrobial agent. This test is usually performed on agar plates. As most of the microorganisms require water for replication, not only the efficacy of CAP on a more or less 'dry' surface is of relevance, but also the bactericidal effect of CAP on bacteria in liquids is of interest. Furthermore—as the bacterial load in wound fluids also plays a major role in wound healing—the influence of the initial cell density in solution on the bactericidal efficacy was assessed. For this purpose, 10^2 – 10^8 cells of *E. coli* in 20 μ l TBS were brought into wells of a 96 well plate and treated with CAP for 1, 2, 3, 4, 5 and 8 min. Afterwards the samples were incubated for 1 h at room temperature, spread on agar plates (in different dilutions) and subsequently incubated at 37 °C for 18 h, so that the surviving bacteria could reproduce and form colonies. Dilutions of untreated bacteria were performed as a control for the initial cell number. The killing efficacy was calculated from the initial cell number and the total count of colony forming units (CFUs).

2.5. Detection of reactive oxygen species: Amplex[®] Red Hydrogen Peroxide Assay

Reactive species are believed to be one part of the plasma which is responsible for killing microorganisms. In CAPs ROS play a crucial role. Recent results show that ROS cause peroxide emergence which finally leads to oxidative damage in the cell wall of the microorganisms [11]. In order to see the correlation between the bactericidal efficacy and the occurrence of reactive species, hydrogen peroxide (H_2O_2) emergence in solution during CAP application was detected with the Amplex[®] Red Hydrogen Peroxide/Peroxidase Assay (Molecular Probes) for several time points. In the presence of peroxidase, the Amplex Red reagent reacts with H_2O_2 in a 1:1 stoichiometry to produce the red-fluorescent oxidation product resorufin. Excitation was detected at 550 nm and emission at 595 nm with a microplate reader (Infinite[®] 200 Pro, Tecan). The Amplex[®] Red Hydrogen Peroxide/Peroxidase Assay was performed according to the manufacturer's protocol with CAP treated bacteria in TBS and TBS alone.

2.6. Detection of reactive nitrogen species

Nitrates and nitrites are products when NO (and other reactive nitrogen species (RNS)) diffuses into liquids. As NO has a very short lifetime, nitrates and nitrites are measured as evidence for emerging RNS in liquids. The Nitrate/Nitrite Colorimetric Assay (Cayman Chemical Company) is based on the reaction of Griess Reagents with nitrates (nitrites are first reduced to nitrates) which then forms a deep purple azo compound. The assay was performed according to the manufacturer's protocol with the supernatants of plasma treated *E. coli* in TBS and TBS alone. The absorbance was measured photometrically at 550 nm with a microplate reader (Infinite[®] 200 Pro, Tecan).

2.7. Reference experiments with hydrogen peroxide (H_2O_2) and nitric oxide (NO)

The synergistic bactericidal effects of NOs and H_2O_2 s have already been examined in the past [22, 26]. To evaluate the influence of dissolved peroxides and products of reactions with NO in liquids, respectively, reference experiments with H_2O_2 (Carl Roth) and a chemical NO donor (DEA NONOate, Sigma Aldrich) were performed. TBS containing 10^4 *E. coli* cells was incubated for one hour with H_2O_2 and DEA NONOate separately and in combination to final concentrations in the range of the measured concentrations after the CAP treatment times of 20 μ l TBS containing *E. coli*. Samples were then spread on agar and incubated overnight at 37 °C. CFUs were counted to control the bacterial reduction.

2.8. Fluorescence proof of intracellular NO

As a final step, direct evidence of the role of RNS in the bactericidal cascade of CAP was presented. 4,5-Diaminofluorescein (DAF-2) is a highly sensitive fluorescent probe for the real-time detection of NO *in vivo*. In the cell, the product reacts rapidly with NO in the presence of O_2 to form the fluorescent compound triazolofluorescein [27, 28]. To detect NO in injured bacteria, 5×10^6 bacteria in 20 μ l TBS were filled in wells of a 96 well plate and treated with CAP for 3 min. After the treatment bacteria were stained with DAF-2 (Enzo Life Sciences) at a final concentration of 10 μ M for 1 h at 4 °C in the dark. Bacteria were fixated on microscope slides and nuclei of bacteria were additionally stained with 10 nM 4', 6-diamidino-2-phenylindole (DAPI, Molecular Probes). As controls, living cells and cells treated with a chemical NO donor (DEA NONOate, Sigma Aldrich) were prepared. Samples were visualized on an Axioimager fluorescence microscope (Zeiss) equipped with a Zeiss AxioCam camera and Zeiss objectives and filters. Light was collected through a 63 \times 0.4 NA water immersion objective. Fluorescence was excited using a 358 nm band pass filter for DAPI and 465–495 nm for Triazolofluorescein. Emission was detected by a 440–480 nm band pass filter (DAPI) and a 505–550 nm band pass filter (Triazolofluorescein). Images were captured from three randomly selected areas for ten different sets of experiments and data were analyzed using Axiovision 4.8 software (Zeiss).

3. Results and discussion

3.1. Cell number tests

As expected the initial cell density of *E. coli* in the liquid had a strong impact on the inactivation efficacy. A time dependence in strong correlation to the cell density was demonstrated (figure 2): up to densities of 10^5 cells per 20 μ l, high reduction rates of up to 5 log steps were achieved in less than 3 min of CAP application. At a concentration of 10^6 cells per 20 μ l, a 6 log reduction was achieved in less than 6 min. In contrast, for higher cell densities above 10^7 cells per 20 μ l the killing efficiency was not time dependent anymore and almost no reduction was measured for CAP treatment times of up to 8 min.

3.2. Peroxides in liquids

The emergence of peroxides in 20 μ l TBS and TBS containing 10^6 *E. coli* after different CAP treatment times was assessed (figure 3). The results clearly show that the content of H_2O_2 in the treated liquids (TBS with/without *E. coli*) increased with longer CAP application times.

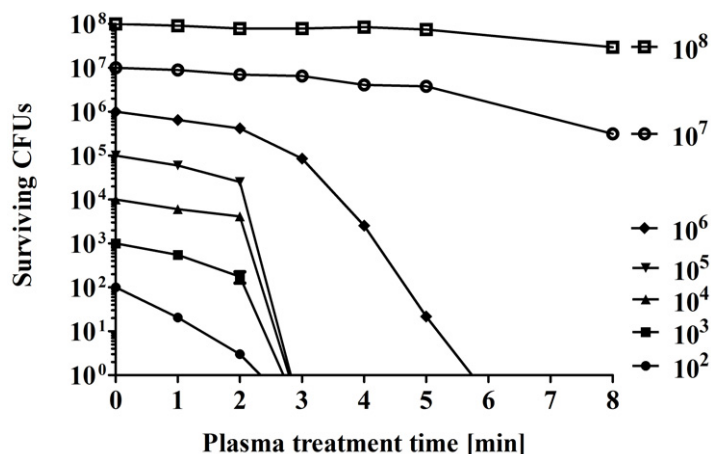


Figure 2. Kinetic inactivation curve of 10^2 – 10^8 *E. coli* cells in $20\ \mu\text{l}$ TBS. The bacteria were treated for 1, 2, 3, 4, 5 and 8 mins with CAP. A 5 log reduction was achieved for 3 min of CAP application for initial cell densities of 10^5 per $20\ \mu\text{l}$ or lower. For cell densities of 10^7 per $20\ \mu\text{l}$ and higher almost no reduction was achieved for CAP treatment times of up to 8 min. By using the logarithmic scale, the depicted error bars—which represent the standard deviation—are very small.

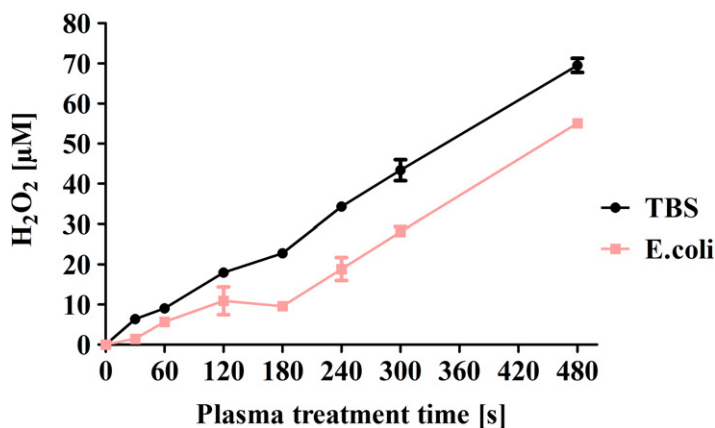


Figure 3. Emergence of peroxides in $20\ \mu\text{l}$ TBS and TBS containing 10^6 *E. coli* after different application times. The peroxide content of TBS and TBS containing *E. coli* increases continuously. In TBS containing *E. coli* the peroxide level is slightly below the level of TBS alone. The error bars show the standard deviation.

However, reference experiments with H_2O_2 show that the measured H_2O_2 concentrations after CAP application are not high enough to inactivate microorganisms (figure 5(a)).

3.3. Nitrates and nitrites in liquids

The total nitrite and nitrate content in $20\ \mu\text{l}$ TBS and TBS containing 10^6 *E. coli* for different CAP application times was measured as described in the experimental setup section (figure 4).

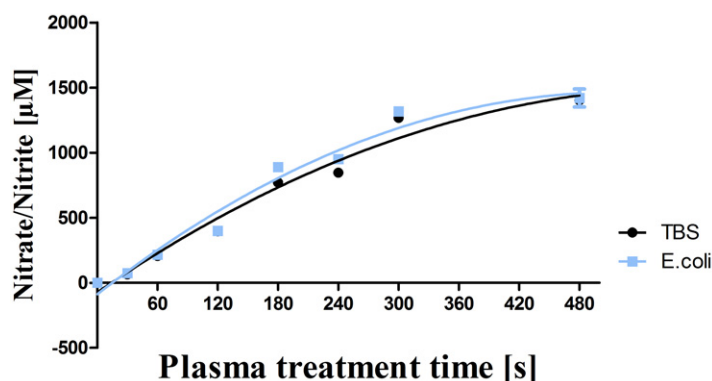


Figure 4. Total nitrite and nitrate content in 20 μl TBS and TBS containing 10^6 *E. coli* after different plasma application times. The nitrate/nitrite level is similar for TBS and TBS containing *E. coli*. The curves are a nonlinear fit to the data. Error bars show the standard deviation. It appears that the nitrate/nitrite concentration may become saturated and there is no reduction when the medium contains *E. coli*—this is in contrast to the hydrogen peroxide concentration shown in figure 3.

The results show that the nitrite and nitrate content of both treated liquids (TBS with/without bacteria) is significantly increased after CAP application: for a treatment time of 4 min (where a 5 log reduction of *E. coli* was achieved) the concentration reached a value of 950 and 1420 μM for a treatment time of 8 min. However, reference experiments with NO possessing concentrations of up to 1500 μM did not reduce bacteria significantly (figures 5(b) and (c)).

3.4. Combination of NO and H_2O_2

Reference experiments with a combined application of NO and H_2O_2 show a much higher inactivation effect on *E. coli* than a treatment with NO or H_2O_2 alone. The concentrations of nitrates and H_2O_2 that were measured after CAP application had no bactericidal effect in the reference experiments with the chemical NO donor NONOate and H_2O_2 (figure 5(a)). But a reduction of 4 log steps can be achieved with 1 mM of NONOate in combination with 1.5 mM of H_2O_2 (figure 5(b)).

3.5. Direct evidence of NO in cells

As described in the experimental setup section a sensitive fluorescent probe (DAF-2) can be used to detect NO in cells in real-time (figure 6): controls of living cells show that *E. coli* cells are not stained by DAF-2 in the absence of a NO-donor. CAP treated bacteria clearly possess green fluorescence in the same way as bacteria, which were treated with a chemical NO-donor. As DAF-2 is only converted to DAF-2T in the presence of NO and O_2 the green fluorescence of CAP treated bacteria is a direct evidence of NO being absorbed by cells during or after plasma application.

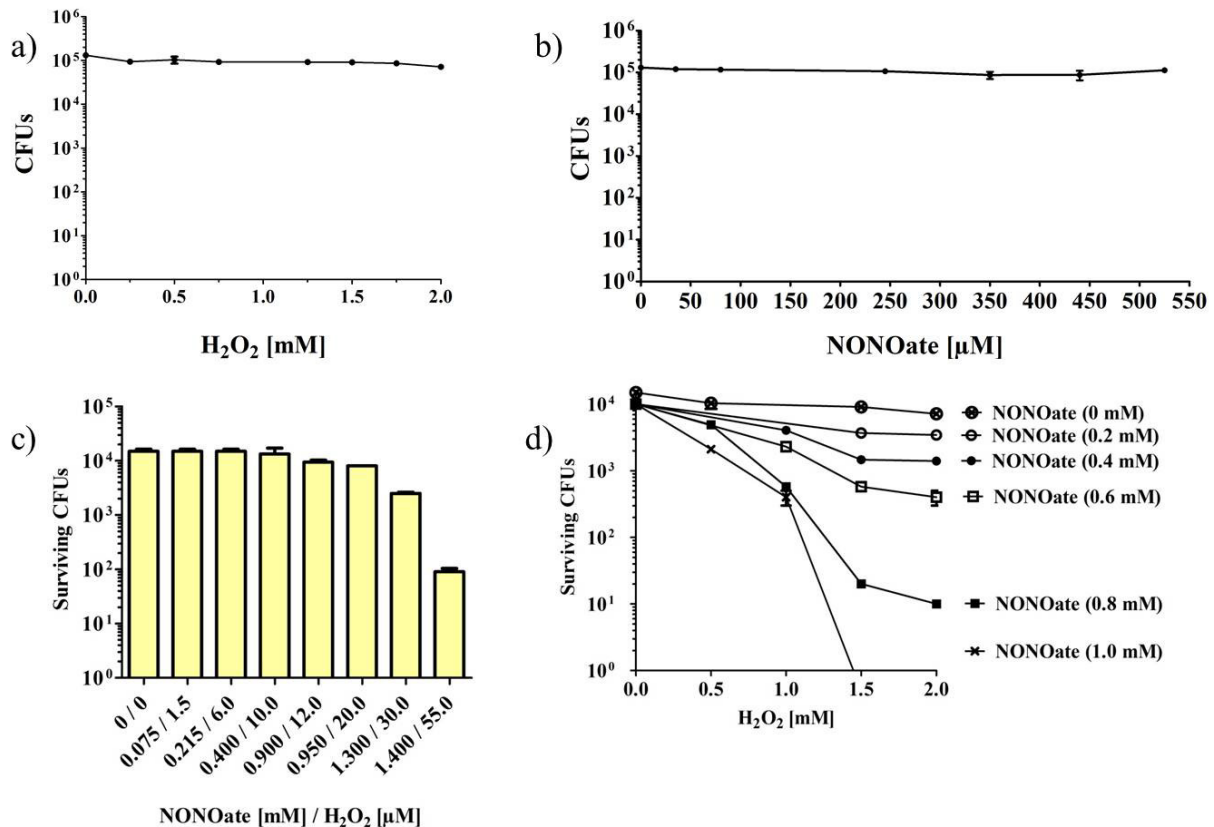


Figure 5. Reference experiments with (a) H₂O₂ alone, (b) NONOate alone and (c) combination of H₂O₂ and NONOate. The concentrations in (c) correspond to those obtained after 1, 2, 3, 4, 5, 6 and 8 min of plasma application. (d) Reference experiments with explicitly higher concentrations of NONOate and H₂O₂.

3.6. Bacteria in solution—model

The model assumptions are the following:

- Bacteria are suspended homogeneously in a solution in which they cannot multiply. The bacterial number density is n_B .
- The plasma is produced at some distance from the surface of the solution. Some non-equilibrium plasma-air reactions produce a number of ROS and RNS, which can be absorbed into the solution. There it can lead to further chemical reactions and can alter the properties of the solution such that it becomes bactericidal. The concentration of such bactericidally reactive species (BRS) in the solution is c_R .
- Their production rate is proportional to the rate at which ROS and RNS are absorbed into the fluid. Let us call this production rate P , where $P \equiv \sum_i n_i v_i A \xi_i$. Here n_i are the densities of ROS/RNS of type i in air, v_i are their velocities (in air), A is the surface area of the suspension which is exposed to the plasma and its chemical products, and all other processes (e.g. absorption efficiency, fluid chemistry, geometrical effects) are summarized in the factor ξ_i . Bacteria have a limited ability to shield themselves against reactive species

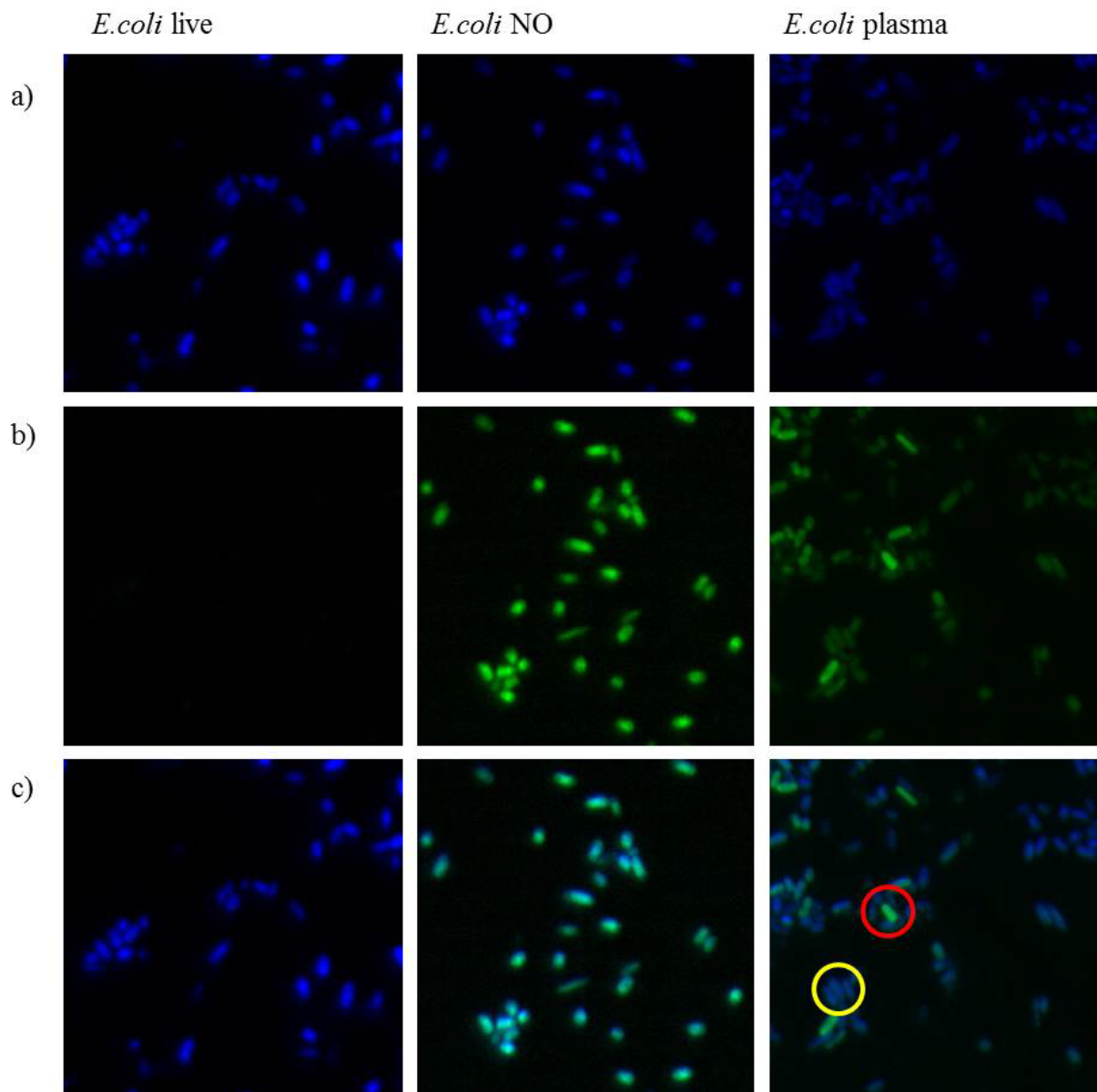


Figure 6. Living *E. coli* cells (*E. coli* live), *E. coli* cells treated with a chemical NO-donor (*E. coli* NO) and *E. coli* cells, treated with plasma for 3 min (*E. coli* plasma). (a) Channel 1: DAPI staining. (b) Channel 2: DAF-2 staining. (c) Channel 1 + 2 merged. Nuclei of all bacteria are stained by DAPI (blue), bacteria that took up NO are stained by DAF-2 (green). Plasma treated bacteria are fluoresce green like those which were treated with a chemical NO donor and in contrast to the untreated, living *E. coli* cells. This means that the plasma treated bacteria took up NO during or as a consequence of the plasma treatment. The merged image of plasma treated *E. coli* clearly shows that the uptake of NO is not regular. The red circle shows a bacterium which took up much more NO than those in the yellow circle.

(e.g. by neutralizing H_2O_2) so that the concentration c_R depends on the bacterial density, as well as the rate P .

The expression governing the concentration c_R is then composed of two parts—a source term proportional to P and a loss term depending on bacterial action:

$$\frac{dc_R}{dt} = \frac{P}{n_M V} - A_B \delta v c_R n_B Q, \quad (1)$$

where $n_M V = Ahn_M$ is the total number of fluid molecules in the suspension (n_M is the molecular density, V is the volume, h the height of the fluid in the vessel—to be precise, we should subtract the volume occupied by the bacteria $= n_B V V_B$, where $n_B V$ is the total number of bacteria and each bacterium has a volume V_B . However, this correction is small and we ignore it). A_B is the surface area of the bacteria ($1.1 \mu\text{m}^2$ for *S. capitis* and $2.6 \mu\text{m}^2$ for *E. coli* [29, 30]), δv is the diffusive drift velocity of the BRS and Q is the conversion efficiency with which the bacteria are able to neutralize these species, i.e. we define the average effect of all the BRS as

$$\delta v Q \equiv \frac{1}{N_S} \sum_i \delta v_i Q_i, \quad (2)$$

where N_S is the total number of BRS present in the suspension.

The next model assumption is that if the concentration c_R of BRS exceeds a certain threshold, c_T , the bacteria cannot cope any more—they become inactivated. The rate at which inactivation proceeds is dose dependent, i.e. proportional to c_R . For simplicity (but not unrealistically) we assume an exponential inactivation rate. Accordingly we put

$$\frac{dn_B}{dt} = -\frac{n_B c_R}{\tau_R} H(c_R - c_T), \quad (3)$$

where $H(c_R - c_T)$ is the Heaviside function (which is 0 for concentrations below the critical value and 1 above this—i.e. this is the simplest mathematical form to specify the threshold requirement above) and τ_R/c_R is the bacterial inactivation time scale. Equations (1) and (3) describe the evolution of the system.

It is convenient to scale c_R with the threshold concentration c_T —i.e. we put

$$c \equiv c_R/c_T \quad (4)$$

and to scale the bacterial density n_B to the initial value n_{B0} —i.e. we put

$$n \equiv n_B/n_{B0} \quad (5)$$

and we scale the time scales with the natural scale $1/A_B \delta v c_T n_{B0} Q$ i.e. we put

$$\tau = t/\tau_B. \quad (6)$$

Then equation (1) becomes

$$\frac{dc}{d\tau} = \frac{c_P}{c_T} - \frac{c}{c_T} n, \quad (7)$$

where we have put $\frac{P\tau_B}{n_M V} \equiv c_P$, the concentration of ROS/RNS produced by the plasma in time τ_B . Equation (3) becomes in these normalized units

$$\frac{dn}{d\tau} = -nc \frac{\tau_B c_T}{\tau_R} H(c - 1). \quad (8)$$

The coupled equations (7) and (8) describe the evolution of the bacterial suspension, n , and the concentration of BRS, c , in the medium as a function of time in response to plasma treatment, given the assumptions stated earlier.

We can examine some special cases:

- (a) Initially, the BRS concentration = 0. As long as $c < 1$ —the concentration of BRS is subcritical.

Then (8) reduces to $\frac{dn}{d\tau} = 0$ and $n = 1$, i.e. the bacterial density remains constant at the initial value. Equation (7) becomes $\frac{dc}{d\tau} = \frac{c_P}{c_T} - \frac{c}{c_T}$. The solution is

$$c = c_P \left(1 - \exp\left(-\frac{\tau}{c_T}\right) \right), \quad (9)$$

i.e. asymptotically $c \rightarrow c_P$. The bacteria are able to ‘protect’ themselves, if $c_P < 1$.

- (b) When the plasma is turned off after a time t_0 , i.e. the BRS concentration has reached a value

$$c_0 = c_P \left(1 - \exp\left(-\frac{\tau_0}{c_T}\right) \right), \quad (10)$$

where $c_0 < 1$.

With the source term turned off, thereafter the BRS concentration evolves according to

$$\frac{dc}{d\tau} = -\frac{c}{c_T} \quad (11)$$

and decreases exponentially as

$$c = c_0 e^{-\tau - \tau_0/c_T}. \quad (12)$$

Throughout this time the bacterial density, n , remains constant.

- (c) In the situation where the concentration τ grows to be larger than 1 (high plasma power and/or longer exposure) then the bacteria cannot protect themselves any longer and they start to die. The bacterial density decreases and self-protection becomes less efficient—a runaway effect sets in until all bacteria are dead. Conversely, increasing the bacteria concentration aids the survival of bacteria—certainly for longer time periods.

Figures 7 and 8 show some sample plots of the temporal evolution of the BRS concentration, c , and the corresponding (normalized) bacterial density, n , as a function of plasma application time. Figure 9 shows what happens when the plasma application is cut off after a certain time. Again, both the evolution of the BRS concentration, c , and the corresponding (normalized) bacterial density, n , are shown. We see that qualitatively the observations (figures 2–4) are reproduced.

In order to obtain some quantitative results, which can then be used for future experiment designs and for possible applications, we note the following:

1. From figure 2 we note that the ‘bifurcation’ in the CFU evolution occurs at initial bacteria densities $10^6 < n_{B0} < 10^7 \text{ cm}^{-3}$. At lower densities the bacteria die after a plasma exposure of the liquid of about 2 min or more.
2. From figure 3 we see that the H_2O_2 concentration (bacteria-free medium) grows linearly. Referring to equation (9) this implies that $\tau/c_T \ll 1$ and hence (9) reduces to $c = \frac{c_P}{c_T} \tau$,

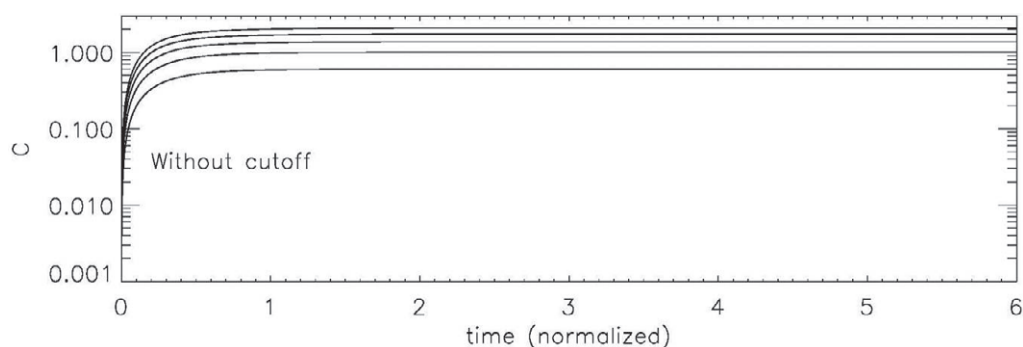


Figure 7. The figure shows the normalized (to a critical threshold value) concentration (c) of BRS inside the medium as function of (normalized) plasma application time for different bacterial loads. The initial bacterial load, n_{B0} , is highest for the lowest curve (in normalized units it decreases from 2.2 in steps of 0.4 to a value of 0.6 for the highest curve). Plasma activation is kept constant. Bacteria are able to reduce the growth of BRS (see text). When the normalized BRS concentration (c) exceeds 1, bactericidal effects take place and the bacterial load is reduced (see figure 2).

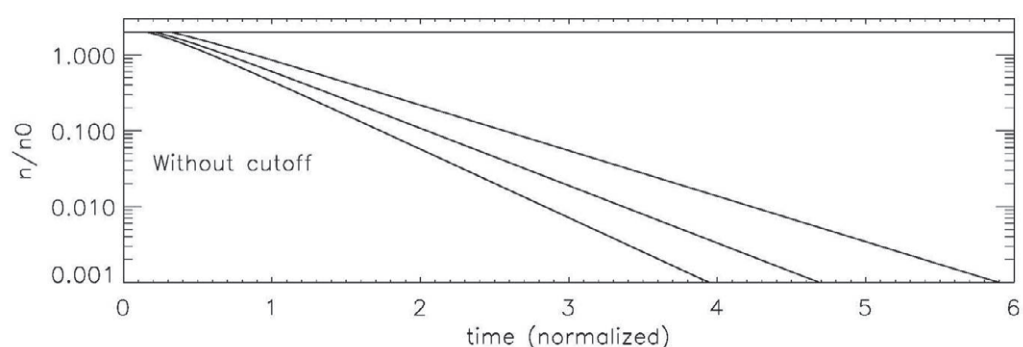


Figure 8. The figure shows the bacterial density (n) inside the medium as a function of time. All values are normalized with respect to the initial bacterial density n_{B0} present before plasma application. The initial bacterial load is lowest for the lowest curve (in normalized units it increases from 0.6 in steps of 0.4 to a value of 2.2 for the highest curve—note that the curves for 1.8 and 2.2 coincide—there is no bactericidal effect from BRS, because the BRS concentration, c , does not exceed the critical value 1—see figure 1). When the BRS level exceeds the critical value ($c = 1$) the bacteria density decreases exponentially in time.

which in unnormalized units becomes

$$c_R = \frac{P}{n_M V} t. \quad (13)$$

From the gradient of figure 3 we obtain

$$\left(\frac{P}{n_M V} \right)_{\text{H}_2\text{O}_2} = 0.167 \quad \mu\text{M s}^{-1}. \quad (14)$$

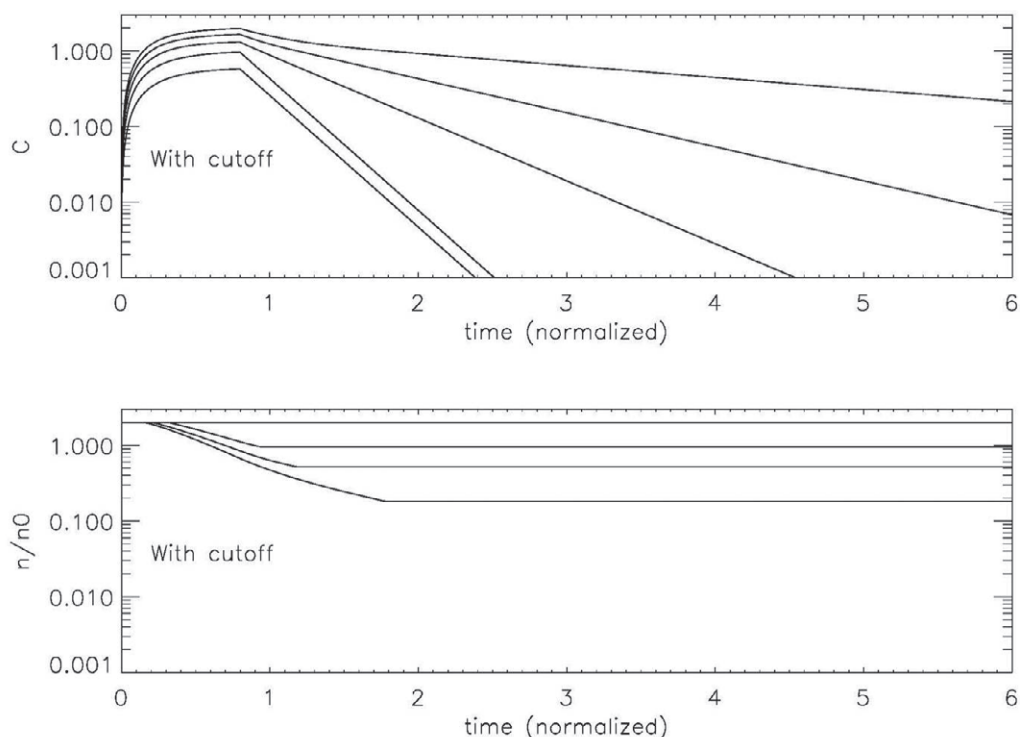


Figure 9. Same as figures 1 and 2 except that the plasma application is cut off after a time t_0 . As the BRS concentration builds up from initially $c = 0$, we see no effect on the bacteria in the suspension. Also, at low initial values of n_{B0} bacteria cannot counteract the growth of BRS concentration and are killed once the concentration exceeds the critical value ($c = 1$). This is seen in the lower three curves (normalized bacterial load 0.6, 1.0 and 1.4 respectively). The BRS concentration then decreases exponentially at rates dependent on the bacterial density. The bacteria density can then reach a reduced threshold value once the BRS density has decreased below the critical value. Comparing this with measurements (figure 2) we see that at the high critical bacteria densities ($>10^6 \text{cm}^{-3}$) lower asymptotic levels (measured after 60 min) are observed, in qualitative agreement with our model.

Similarly, from figure 4 we obtain an initial growth

$$\left(\frac{P}{n_M V} \right)_{\text{Nitrites/Nitrates}} = 3.8 \quad \mu\text{M s}^{-1}. \quad (15)$$

with a saturation time scale of ~ 300 s.

3. An equivalent effect to that of figure 2 is observed in figure 3 as well. Here a bacterial density of 10^6cm^{-3} was used and compared with the bacteria-free medium. Whilst the H_2O_2 concentration increases linearly with plasma application time (i.e. saturation has not yet been reached after 8 min) in the bacteria-free medium, there is a clear inhibition signature once the medium contains bacteria—up to plasma application times of 2 min.

Therefore the H_2O_2 concentration follows the bacteria-free trend. Comparison with figure 2 ($n_b = 10^6 \text{ cm}^{-3}$) shows that the bacterial load has been reduced by a factor of 10 after 3 min plasma application—apparently $n_b = 10^6 \text{ cm}^{-3}$ is just too small for the ‘self-protection’ process described here to remain effective.

4. No bacteria-related effect is seen for the same conditions for dissolved nitrites and nitrates. The observed self-saturation is most likely chemical in origin. This suggests (not unexpectedly) that the ‘self-protection’ process depends in detail on the chemical products in the medium. This in turn implies that our ‘one-component model’ (which assumes one dominant process) may be too simple and further developments of the model are necessary.
5. From the observations of figure 2, the ‘bifurcation’ in the bacteria survival curves occurs for initial bacteria densities $n_{B0} \approx 10^6 \text{ cm}^{-3}$. Also, the rapid bactericidal effect sets in at low bacterial densities after 2 min of plasma treatment. The latter observation implies

$$c_R = \frac{pt_B}{n_M V} \approx c_T \quad \text{when } t_B = 2 \text{ min.} \quad (16)$$

In other words, the critical concentration for $\text{H}_2\text{O}_2 = c_T/\text{H}_2\text{O}_2 \approx 20 \mu\text{M}$. The former observation implies that the neutralization of BRS by bacterial action requires (see equation (1))

$$A_B \delta V c_R n_{B0} Q > \frac{P}{n_M V}, \quad (17)$$

where we may put $c_R = c_T$ to obtain the threshold value for the initial bacterial density n_{B0} .

Substituting (16) yields

$$\delta v Q > \frac{1}{A_B} n_{B0} t_B. \quad (18)$$

For *E. coli* this gives $\delta v Q > 0.32 \text{ cm s}^{-1}$. The molecular diffusivity in fluids yields mean diffusive speeds of $= 3\kappa/\lambda$, where κ is the diffusion coefficient and λ the mean free path. Typical values for water give $\delta v \simeq \text{cm s}^{-1}$, so that we obtain a ‘conversion efficiency’, $Q \gtrsim 0.3$.

In conclusion, the simple model we have presented here is able to reproduce all the qualitative features of the observations. The measurements can be used to derive properties of the plasma–medium interaction as well as the bacterial ‘self-protection’ limits. Further improvements of the model, involving detailed features of the plasma–liquid chemistry are possible.

3.7. Discussion and conclusions

The use of CAPs in medicine and health care as a disinfecting agent would solve many problems—starting from irritated skin because of washing and disinfecting hands, in sterilizing surgical equipment, up to the prevention of nosocomial infections and spread of resistant microorganisms. A large number of studies performed in recent years showed that all tested pathogens could be easily inactivated by CAP within small time scales [1–7, 31].

There are several research groups worldwide which use different plasma production techniques—and all devices produce different plasmas i.e. different compositions and concentrations of electrons, charged particles, reactive species, etc. The CAP device used for

this study produces plasma in air. Our diagnostic measurements showed that UV and heating effects can be neglected and that the bactericidal effect must be due to charged particles and reactive species. Recent studies mainly focused on oxidative damage on bacteria by neutral active species, either stable ones, e.g. ozone and H_2O_2 , or short-lived ROS, such as hydroxyl radicals and atomic oxygen [32]. But although Gram negative bacteria like *E. coli* do not possess an appreciable amount of catalases/peroxidases [33] preliminary results showed that ROS cannot be the only bactericidal agent in CAPs. It was reported that lipid peroxidation after CAP treatment of *E. coli* occurs due to emerging peroxides in liquids [11]. But there are other mechanisms which lead to lipid peroxidation, too. While NO itself appears to inhibit the propagation of lipid peroxidation (by scavenging peroxy radicals), [34] the highly oxidizing peroxynitrite can react with unsaturated fatty acids and initiate lipid peroxidation directly, through scavenging of antioxidants, or by reaction with low-density lipoproteins [35–38]. This is consistent with Brun *et al* [39] who showed that scavenging ROS with, for example, *N*-acetylcystein (NAC) does not influence the bactericidal efficacy of plasma distinctly. Our experiments demonstrate the uptake of NO in *E. coli* and that furthermore NO is produced in a sufficient amount to increase its oxidation products nitrite and nitrate in solution. Nevertheless control experiments clearly demonstrate that high concentrations of neither H_2O_2 nor NO and its oxidation products are individually able to inactivate *E. coli* significantly. For comparison, to disinfect contact lenses with H_2O_2 a 3% (880 mM, e.g. Oxysept[®]) solution is used—a 15 000 times higher concentration than obtained after 8 min of plasma application (55 μM). Furthermore, of course, NO itself cannot be used as a superficial disinfectant. In addition it is known that only a combination of NO and H_2O_2 has a markedly bactericidal effect and that NO is relatively unreactive at physiological (nM) concentrations. Its reactivity increases for higher concentrations (low μM), such as would occur in biological membranes or upon inflammatory release of NO [22, 26, 36]. These findings were confirmed in our control experiments, where only higher concentrations of nitrates and H_2O_2 (in the mM range) than measured after CAP application, showed a bacterial reduction of 4 log steps. It is therefore reasonable to suppose that the high bactericidal effect of CAP is due to an interaction of both—ROS and RNS.

When we remember the possible application areas of CAP we have surface/hand disinfection, sterilization of, for example, surgical instruments and even wound disinfection in mind. Until today chemicals and topical drugs are the standard way for treatment. Consequently all these areas are firmly linked with high costs, high environmental pollution/waste or adverse health effects. To use a device which utilizes the surrounding air could therefore be a very attractive alternative.

Nevertheless further investigations of the chemistry in solution after CAP application have to be carried out to study the bactericidal mechanisms—besides the density effect—as well as the effects of CAPs on eukaryotic cells before implementing clinical trials for disinfecting hands or wounds.

Acknowledgments

We would like to thank Professor Hans-Ulrich Schmidt for providing the stock cultures of *E. coli* and *S. capitis* and Andrea Schäfer for fruitful discussions. This study was supported by the Max-Planck Society under grant M.TT.A.Ext00002.

References

- [1] Morfill G E, Shimizu T, Steffes B and Schmidt H U 2009 Nosocomial infections—a new approach towards preventive medicine using plasmas *New J. Phys.* **11** 115019
- [2] Daeschlein G, Scholz S, von Woedtke T, Niggemeier M, Kindel E, Brandenburg R, Weltmann K D and Junger M 2011 In vitro killing of clinical fungal strains by low-temperature atmospheric-pressure plasma jet *IEEE Trans. Plasma Sci.* **39** 815–21
- [3] Maisch T, Shimizu T, Isbary G, Heinlin J, Karrer S, Klampfl T G, Li Y F, Morfill G and Zimmermann J L 2012 Contact-free inactivation of *Candida albicans* biofilms by cold atmospheric air plasma *Appl. Environ. Microbiol.* **78** 4242–7
- [4] Zimmermann J L, Dumler K, Shimizu T, Morfill G E, Wolf A, Boxhammer V, Schlegel J, Gansbacher B and Anton M 2011 Effects of cold atmospheric plasmas on adenoviruses in solution *J. Phys. D: Appl. Phys.* **44** 505201
- [5] Hähnel M, von Woedtke T and Weltmann K-D 2010 Influence of the air humidity on the reduction of bacillus spores in a defined environment at atmospheric pressure using a dielectric barrier surface discharge *Plasma Process. Polym.* **7** 244–9
- [6] Klampfl T G, Isbary G, Shimizu T, Li Y F, Zimmermann J L, Stolz W, Schlegel J, Morfill G E and Schmidt H U 2012 Cold atmospheric air plasma sterilization against spores and other microorganisms of clinical interest *Appl. Environ. Microbiol.* **78** 5077–82
- [7] Zimmermann J L, Shimizu T, Schmidt H-U, Li Y-F, Morfill G E and Isbary G 2012 Test for bacterial resistance build-up against plasma treatment *New J. Phys.* **14** 073037
- [8] Maisch T, Shimizu T, Li Y-F, Heinlin J, Karrer S, Morfill G and Zimmermann J L 2012 Decolonisation of MRSA, *S. aureus* and *E. coli* by cold-atmospheric plasma using a porcine skin model *in vitro PLoS One* **7** e34610
- [9] Maisch T, Shimizu T, Mitra A, Heinlin J, Karrer S, Li Y F, Morfill G and Zimmermann J L 2012 Contact-free cold atmospheric plasma treatment of *Deinococcus radiodurans* *J. Ind. Microbiol. Biotechnol.* **39** 1367–75
- [10] Zimmermann J L, Shimizu T, Boxhammer V and Morfill G E 2012 Disinfection through different textiles using low-temperature atmospheric pressure plasma *Plasma Process. Polym.* **9** 792–8
- [11] Joshi S G, Cooper M, Yost A, Paff M, Ercan U K, Fridman G, Friedman G, Fridman A and Brooks A D 2011 Nonthermal dielectric-barrier discharge plasma-induced inactivation involves oxidative DNA damage and membrane lipid peroxidation in *Escherichia coli* *Antimicrob. Agents Chemother.* **55** 1053–62
- [12] Nosenko T, Shimizu T and Morfill G E 2009 Designing plasmas for chronic wound disinfection *New J. Phys.* **11** 115013
- [13] Traylor M J, Pavlovich M J, Karim S, Hait P, Sakiyama Y, Clark D S and Graves D B 2011 Long-term antibacterial efficacy of air plasma-activated water *J. Phys. D: Appl. Phys.* **44** 472001
- [14] Kong M G, Kroesen G, Morfill G, Nosenko T, Shimizu T, Dijk J V and Zimmermann J L 2009 Plasma medicine: an introductory review *New J. Phys.* **11** 115012
- [15] Shimizu T, Nosenko T, Morfill G E, Sato T, Schmidt H U and Urayama T 2010 Characterization of low-temperature microwave plasma treatment with and without UV light for disinfection *Plasma Process. Polym.* **7** 288–93
- [16] Laroussi M 2005 Low temperature plasma-based sterilization: overview and state-of-the-art *Plasma Process. Polym.* **2** 391–400
- [17] Laroussi M 2002 Nonthermal decontamination of biological media by atmospheric-pressure plasmas: review, analysis and prospects *IEEE Trans. Plasma Sci.* **30** 1409–15
- [18] Laroussi M, Mendis D A and Rosenberg M 2003 Plasma interaction with microbes *New J. Phys.* **5** 341
- [19] Laroussi M and Leipold F 2004 Evaluation of the roles of reactive species, heat and UV radiation in the inactivation of bacterial cells by air plasmas at atmospheric pressure *Int. J. Mass Spectrom.* **233** 81–6

- [20] Pompl R *et al* 2009 The effect of low-temperature plasma on bacteria as observed by repeated AFM imaging *New J. Phys.* **11** 115023
- [21] Kvam E, Davis B, Mondello F and Garner A L 2012 Nonthermal atmospheric plasma rapidly disinfects multidrug-resistant microbes by inducing cell surface damage *Antimicrob. Agents Chemother.* **56** 2028–36
- [22] Miller R A and Britigan B E 1997 Role of oxidants in microbial pathophysiology *Clin. Microbiol. Rev.* **10** 1–18
- [23] Joshi S G, Paff M, Friedman G, Fridman G, Fridman A and Brooks A D 2010 Control of methicillin-resistant *Staphylococcus aureus* in planktonic form and biofilms: a biocidal efficacy study of nonthermal dielectric-barrier discharge plasma *Am. J. Infect. Control* **38** 293–301
- [24] Kogelschatz U 2003 Dielectric-barrier discharges: their history, discharge physics and industrial applications *Plasma Chem. Plasma Process.* **23** 1–46
- [25] Shimizu T, Zimmermann J L and Morfill G E 2011 The bactericidal effect of surface micro-discharge plasma under different ambient conditions *New J. Phys.* **13** 023026
- [26] Pacelli R, Wink D A, Cook J A, Krishna M C, DeGraff W, Friedman N, Tsokos M, Samuni A and Mitchell J B 1995 Nitric oxide potentiates hydrogen peroxide-induced killing of *Escherichia coli* *J. Exp. Med.* **182** 1469–79
- [27] Kojima H, Nakatsubo N, Kikuchi K, Kawahara S, Kirino Y, Nagoshi H, Hirata Y and Nagano T 1998 Detection and imaging of nitric oxide with novel fluorescent indicators: diaminofluoresceins *Anal. Chem.* **70** 2446–53
- [28] Kojima H, Sakurai K, Kikuchi K, Kawahara S, Kirino Y, Nagoshi H, Hirata Y, Akaike T, Maeda H and Nagano T 1997 Development of a fluorescent indicator for the bioimaging of nitric oxide *Biol. Pharm. Bull.* **20** 1229–32
- [29] Miao J, Hodgson K O, Ishikawa T, Larabell C A, LeGros M A and Nishino Y 2003 Imaging whole *Escherichia coli* bacteria by using single-particle x-ray diffraction *Proc. Natl Acad. Sci.* **100** 110–2
- [30] Amako K and Umeda A 1977 Scanning electron microscopy of staphylococcus *J. Ultrastruct. Res.* **58** 34–40
- [31] Tseng S, Abramzon N, Jackson J O and Lin W J 2012 Gas discharge plasmas are effective in inactivating *Bacillus* and *Clostridium* spores *Appl. Microbiol. Biotechnol.* **93** 2563–70
- [32] Dobrynin D, Friedman G, Fridman A and Starikovskiy A 2011 Inactivation of bacteria using dc corona discharge: role of ions and humidity *New J. Phys.* **13** 103033
- [33] Welch R A 2006 The genus *Escherichia* *Proteobacteria: Gamma Subclass* (New York: Springer) pp 60–71
- [34] d’Ischia M, Palumbo A and Buzzo F 2000 Interactions of nitric oxide with lipid peroxidation products under aerobic conditions: inhibitory effects on the formation of malondialdehyde and related thiobarbituric acid-reactive substances *Nitric Oxide* **4** 4–14
- [35] Hogg N and Kalyanaraman B 1999 Nitric oxide and lipid peroxidation *Biochim. Biophys. Acta* **1411** 378–84
- [36] Carré J, Singer M and Moncada S 2007 Mechanisms of sepsis-induced organ dysfunction and recovery *Update in Intensive Care and Emergency Medicine* ed E Abraham and M Singer (Berlin: Springer) pp 77–95
- [37] Rubbo H, Radi R, Trujillo M, Telleri R, Kalyanaraman B, Barnes S, Kirk M and Freeman B A 1994 Nitric oxide regulation of superoxide and peroxynitrite-dependent lipid peroxidation. Formation of novel nitrogen-containing oxidized lipid derivatives *J. Biol. Chem.* **269** 26066–75
- [38] Darley-Usmar V M, Patel R P, O’Donnell V B and Freeman B A 2000 Antioxidant actions of nitric oxide *Nitric Oxide* ed J I Louis (San Diego: Academic) pp 265–76
- [39] Brun P *et al* 2012 Disinfection of ocular cells and tissues by atmospheric-pressure cold plasma *PLoS One* **7** e33245